Published in final edited form as:
Clin Cancer Res. 2010 December 1; 16(23): 5722–5733. doi:10.1158/1078-0432.CCR-10-1693.

Intratumoral mediated immunosuppression is prognostic in genetically engineered murine models of glioma and correlates to immune therapeutic responses

Ling-Yuan Kong[1,*], **Adam S. Wu**[1,*], **Tiffany Doucette**[1], **Jun Wei**[1], **Waldemar Priebe**[2], **Gregory N. Fuller**[3], **Wei Qiao**[4], **Raymond Sawaya**[1], **Ganesh Rao**[1,*], and **Amy B. Heimberger**[1,*]

[1]Department of Neurosurgery, The University of Texas M. D. Anderson Cancer Center, Houston, TX

[2]Department of Experimental Therapeutics, The University of Texas M. D. Anderson Cancer Center, Houston, TX

[3]Department of Neuropathology, The University of Texas M. D. Anderson Cancer Center, Houston, TX

[4]Department of Biostatistics, The University of Texas M. D. Anderson Cancer Center, Houston, TX

Abstract

Purpose—Pre-clinical murine model systems used for the assessment of therapeutics have not been predictive of human clinical responses, primarily because their clonotypic nature does not recapitulate the heterogeneous biology and immunosuppressive mechanisms of humans. Relevant model systems with mice that are immunologically competent are needed to evaluate the efficacy of therapeutic agents, especially immunotherapeutics.

Experimental Design—Using the RCAS/Ntv-a system, mice were engineered to co-express platelet-derived growth factor receptor (PDGF)-B + B-cell lymphoma (*Bcl*)-*2* under the control of the glioneuronal-specific *Nestin* promoter. The degree and type of tumor-mediated immunosuppression was determined in these endogenously arising gliomas based upon the presence of macrophages and regulatory T cells (Tregs). The immunotherapeutic agent, WP1066, was tested *in vivo* to assess therapeutic efficacy and immune modulation.

Results—*N-tva* mice were injected with RCAS vectors to express PDGF-B + *Bcl-2*, resulting in both low- and high-grade gliomas. Consistent with observations in human high-grade gliomas, mice with high-grade gliomas also developed a marked intratumoral influx of macrophages that was influenced by tumor signal transducer and activator of transduction (STAT) 3 expression. The presence of intratumoral F4/80 macrophages was a negative prognosticator for long-term survival. In mice expressing both PDGF-B + *Bcl-2* that were treated with WP1066, there was 55.5%

Corresponding author: Amy B. Heimberger, Department of Neurosurgery, The University of Texas M. D. Anderson Cancer Center, Unit 442, 1515 Holcombe Boulevard, Houston TX 77030-4009 USA. Phone: 713-792-2400; Fax: 713-794-4950; aheimber@mdanderson.org or Ganesh Rao, Department of Neurosurgery, The University of Texas, M.D. Anderson Cancer Center, Unit 442, 1515 Holcombe Boulevard, Houston, TX 77030-4009 USA. Phone: 713-192-2400; Fax 713-794-4950; grao@mdanderson.org.
*co-lead and co-senior authors

Disclosure of Potential Conflicts of Interest
W. Priebe and A. B. Heimberger hold patents and have a financial interest in the development of WP1066.

increase in median survival time ($P < 0.01$), with an associated inhibition of intratumoral STAT3 and macrophages.

Conclusions—Although randomization is necessary for including mice in a therapeutic trial, these murine model systems are more suitable for testing therapeutics, and especially immune therapeutics, in the context of translational studies.

Keywords

Gliomas; signal transducer and activator of transcription 3; macrophages; Tregs

Introduction

The extrapolation of preclinical data, using murine models to determine clinical efficacy of novel therapeutics is confounded by many issues including, but not limited to, immunologically incompetent model systems and clonotypic tumors that do not fully recapitulate the heterogeneous nature of human tumors (1,2). Additionally, many experimental cell lines, by being perpetuated *in vitro* (in some cases for decades), have significantly diminished immunosuppressive properties when compared with the phenotype and function of cancer cells isolated immediately from human tumors (3). Ideally, screening immunotherapeutic approaches for clinical trial implementation should be selected for robust responses in immunocompetent murine model systems in which the murine gliomas correlate with the biology of human malignant gliomas (4–6). The use of genetically engineered mouse models of malignancy has been shown to simulate human responses within the context of clinical trials (7,8) and thus provides distinct advantages for evaluating immune prognostic factors and immunotherapeutics.

Ligand interaction of the platelet-derived growth factor receptor (PDGFR)-B, which is over-expressed in human malignant gliomas (9,10), results in activation of pro-survival signaling pathways that promote tumor cell growth (11). Murine model systems have demonstrated that over-expression of PDGF-B in the brain induces grade II/III oligodendroglioma (12). Other genes, such as the antiapoptotic B-cell lymphoma (*Bcl*)-*2*, have been shown to cooperate with PDGF-B to enhance tumor formation and promote progression to a higher grade tumor (13–15). PDGF-B, upon ligand binding and in a manner dependent on Src kinase activity, rapidly phosphorylates and activates signal transducer and activator of transduction (STAT)3, forming p-STAT3 (16). Under normal physiological conditions, STAT3 activation depends on ligand-receptor interaction, primarily under the control of growth factor receptor tyrosine kinases or cytokine and G-protein receptors with associated Janus kinase-2 (17,18). However, in cancer cells, these tyrosine kinases are among the most frequently activated oncogenic proteins. STAT3 has been shown to be persistently activated in most human cancers, including gliomas (19). STAT3 activation entails protein phosphorylation at the tyrosine-705 site (p-STAT3), dimerization, nuclear translocation, and subsequent binding to consensus promoter sequences of target genes, thus initiating transcription of many genes implicated in tumorigenesis including *Bcl-2* (20–22). Overall, the STAT3 pathway mediates a transcriptional response favoring tumor survival, proliferation and angiogenesis (23).

Tumor-expressed STAT3 also induces STAT3 expression in a variety of immune cells, resulting in global immunosuppression (24). STAT3 expression in macrophages inhibits their activation (25) and induces a polarization from the effector M1 phenotype to the immunosuppressive M2 phenotype (26,27). Moreover, STAT3 expression can reduce the cellular cytotoxicity of natural killer cells and neutrophils, as well as the expression of MHC II, CD80, CD86, and IL-12 in dendritic cells, rendering them unable to activate T cells and

to generate antitumor immunity (28). Furthermore, STAT3 has been shown to be a transcriptional regulator of forkhead box protein (FoxP3) (29) and Treg functional activity (30). Finally, STAT3 has been shown to maintain the proliferation and multipotency in glioma cancer stem cells (31), including their immunosuppressive properties (32). Cumulatively, these data indicate that the STAT3 pathway is a key molecular hub in tumor-mediated immunosuppression.

STAT3, and its down-stream regulated genes such as *Bcl-2*, can be blocked with WP1066 (33), an orally bioavailable small molecule inhibitor with excellent CNS penetration and minimal dose-limiting toxicity (34). WP1066 can exert direct anti-tumor activity including the induction of caspase-dependent apoptotic cell death in (33,35,36) and inhibition of angiogenesis (37). Moreover, WP1066 is a potent inducer of pro-inflammatory (38) responses and can reverse the functional immunosuppression of macrophages (39) and glioma cancer stem cells (32). To study tumor-induced immunosuppression in endogenously arising gliomas, we used the RCAS/*Ntv-a* transgenic mouse system. In this system, a gene is cloned into a modified avian retrovirus (RCAS) that is replication-defective in mammalian cells. The vector is introduced into *Ntv-a* mice that express TVA (avian leukosis virus subtype A receptor, the receptor for RCAS) under control of the *Nestin* promoter. Nestin-positive cells include glioneuronal precursors, the presumed cells of origin for glial tumors (5,40). The gene is incorporated into the cell's genome and is expressed driven by the constitutive retroviral promoter, long terminal repeat (LTR). This method of somatic cell gene transfer has been used to assess gene over-expression *in vivo* and to model various brain tumors (41–43). We used this model to co-express PDGF-B and *Bcl-2*. *Bcl-2* lies downstream in the STAT3 signaling pathway making tumors formed by the co-expression of PDGF-B + *Bcl-2* relevant to the study of STAT3 biology. Because Ntv-a mice are immunocompetent, they are ideal for the study of immunosuppression induced by these gliomas. Most current murine model systems use either immunodeficient mice with human tumor xenografts or syngeneic clonotypic cell lines which make it difficult, if not impossible, to appreciate the immunological influence on tumor biology in the native animal.

We hypothesized that the gliomas formed in *Ntv-a* mice are immunosuppressive, that the high-grade gliomas would be more immunosuppressive relative to the low-grade gliomas, and that this model of endogenously arising malignant gliomas could be used to test immunotherapeutics. Here, we show that constitutive expression of PDGF-B + *Bcl-2* in this model system induces intratumoral Tregs and macrophages, similar to the induction of these cells observed in human malignant gliomas. We also show that this model system can be exploited for testing immune therapeutics.

Materials and Methods

Vector constructs

The RCAS-Bcl-2 vector was a gift of Dr. Daniel Fults (University of Utah) and the details of its creation are described in (44). Briefly, this vector was constructed by ligating a PCR-generated cDNA corresponding to the entire coding sequence of human *Bcl-2* into the retroviral vector RCASBP. RCAS-PDGF-B was a gift of Dr. Wei Zhang (M.D. Anderson Cancer Center), and the details of its creation are described (45).

Transfection of DF-1 cells

Live virus was produced using the plasmid versions of the RCAS vectors transfected into DF-1 immortalized chicken fibroblasts (grown in DMEM medium containing 10% FBS

[GIBCO, Carlsbad, CA] in a humidified atmosphere of 95% air/5% CO2 at 37°C), using FuGene6 (Roche, Nutley, NJ).

Verification of transgene expression

Bcl-2 expression after infection with RCAS-*Bcl-2* was verified by exposing un-transfected DF-1 cells (cultured to 50% confluency) for 48 hours to filtered medium conditioned by DF-1/RCAS-*Bcl-2*-transfected cells. Cells were then fixed with 4% paraformaldehyde in PBS followed by treatment with cold methanol, and immunocytochemical labeling was performed by standard methods, using a mouse monoclonal antibody against human *Bcl-2* (1:200; Santa Cruz Biotechnology, Santa Cruz, CA) and goat anti-mouse Alexa Fluor® 594 fluorescent conjugate (1:500; Molecular Probes, Carlsbad, CA) for detection. After mounting and labeling of cell nuclei with Prolong Gold antifade reagent with DAPI (Molecular Probes, Carlsbad, CA), staining was examined using a Zeiss Axioskop 40 microscope. Verification of PDGF-B expression from DF-1 cells after infection was performed by Western blot. Whole-cell lysates were prepared from DF-1 cell cultures 48 hours after infection with virus-containing medium conditioned by DF-1 cells expressing RCAS-PDGF-B. Protein samples (10 μg) were fractionated by SDS-PAGE using gels containing 10% polyacrylamide, transferred to PVDF membrane, and probed with the anti-HA antibody (1:1000; F7, Santa Cruz Biotechnology, Santa Cruz, CA) to detect PDGF-B expression. Secondary antibody used for detection was goat anti-mouse IgG (1:2500; Pierce, Rockford, IL). The blots were developed with the ECL Plus Detection Kit (GE Healthcare, Piscataway, NJ) following manufacturer protocol.

In vivo somatic cell transfer in transgenic mice

Creation of the transgenic Ntv-a mouse has been previously described (46). The mice are mixtures of the following strains: C57BL/6, BALB/C, FVB/N, and CD1. To transfer genes via RCAS vectors, transfected DF-1 producer cells (1×10^5 cells in 1 to 2 μL of PBS) were injected into the right frontal brain lobe of Ntv-a mice from an entry point just anterior to the coronal suture of the skull using a 10 μl gas-tight Hamilton syringe. Mice were injected within 24 to 72 hours after birth because the population of Nestin-positive cells producing TVA receptors diminishes progressively with time. For co-injection of RCAS-PDGF-B and RCAS-Bcl-2 equal numbers of DF-1 cells were injected. The mice were sacrificed 90 days after injection or sooner if they demonstrated neurological morbidity related to tumor burden, including hydrocephalus or disability. The brains were fixed in formalin, embedded in paraffin, sectioned for immunohistochemical analysis, and analyzed for tumor formation. Histological verification of tumor formation and determination of low- or high-grade type was performed by the study neuropathologist (GNF). High-grade tumors were differentiated by the presence of microvascular proliferation, mitotic activity, and necrosis. The animal experiments described in this research were approved by The Institutional Animal Care and Use Committee at The University of Texas M. D. Anderson Cancer Center (Protocol 08-06–11632 and 08-06–11832).

Immunohistochemistry

Formalin-fixed, paraffin-embedded 4μm sections of the glioma were first deparaffinized in xylene and rehydrated in ethanol. Endogenous peroxidase was blocked with 0.3% hydrogen peroxide/methanol for 10 min at room temperature. Then, the ThermoScientific PTModule (Thermo Fisher Scientific, Fremont, CA) with citrate buffer (pH 6.0) was used for antigen retrieval. Immunohistochemical staining was performed using the Lab Vision Immunohistochemical Autostainer 360 (Thermo Fisher Scientific, Fremont, CA). The staining was visualized using an avidin-biotin complex technique with diaminobenzidine (Invitrogen, Carlsbad, CA) as the chromogenic substrate and hematoxylin as the counterstain. A mouse monoclonal anti-HA antibody (1:50; Santa Cruz Biotechnology,

Santa Cruz, CA) was used to detect the HA epitope tag on the PDGF-B gene. To detect expression of human Bcl-2 expressed by RCAS, we used a primary monoclonal antibody specific for human Bcl-2 (1:100; Santa Cruz Biotechnology, Santa Cruz, CA). To detect GFAP expression, a rabbit polyclonal anti-GFAP antibody was used (1:500; DAKOCytomation, Carpinteria, CA). To detect p-STAT3 expression, we used a rabbit polyclonal anti-p-STAT3 (Tyr705) antibody (1:50; Cell Signaling Technology, Danvers, MA). To detect expression of the macrophage-restricted cell surface glycoprotein F4/80, a purified anti-mouse F4/80 (1:50; Biolegend, San Diego, CA) antibody was used. To detect FoxP3 expression, a purified mouse anti-FoxP3 antibody (1:50; Biolegend, San Diego, CA) was used.

Two independent observers (L-YK, AW) quantitatively evaluated p-STAT3, FoxP3, and F4/80 expression by analyzing the tumors using high-power fields (max: x400 objective and x100 eyepiece) of each specimen in the regions with the highest relative positive staining for that individual specimen. The analysis was reviewed again by the neuropathologist (GNF). The observers examined each tumor in a blinded fashion and in duplicate. Each observer recorded the absolute number of cells with positive staining. The duplicate numbers were then averaged for the final number of cells with positive expression per specimen.

Mitotic index

To detect and quantify mitotic activity, formalin-fixed, paraffin-embedded, tumor-bearing tissue sections were immunostained with an antibody against pHH3. The number of positively stained cells in the area of highest tumor cell density were counted in ten non-overlapping high-power microscopic fields (400X magnification) from five different tumor-bearing brains from the RCAS-PDGF-B and RCAS-PDGF-B + RCAS-Bcl-2 mice. The mitotic index was calculated as the number of positive cells divided by the number of total cells in each field. The median number of cells counted was 1795 (range 616 – 3003).

STAT3 inhibitor

WP1066 which blocks p-STAT3 was synthesized and supplied by Dr. Waldemar Priebe (M. D. Anderson). WP1066 was dissolved in dimethylsulfoxide (DMSO, Sigma-Aldrich, St Louis, MO) as a stock solution and serially diluted to the desired concentration with RPMI 1640 medium.

Treatment schema and animal randomization

After receiving the injection of the PDGF-B + *Bcl-2* constructs as described, littermates were randomized to the treatment or control groups. Twenty-one days after introduction of the glioma-inducing transgenes, treatment was started with WP1066, administered by oral gavage (o.g.) in a vehicle of DMSO/PEG300 (20 parts/80 parts) on a q.i.d. schedule (5 days on, 2 days off) for a total of three weeks. Fifteen mice per experimental group were used including treatment with the DMSO/PEG300 vehicle alone in the control group. This methodology of using RCAS/Ntv-a mice to determine treatment efficacy has been described previously (47).

Statistics

Kaplan-Meier product-limit survival probability estimates of overall survival were calculated (48) and log-rank tests (49) were performed to compare overall survival times between treatment groups and the control arm. Ex-vivo or in vitro data are presented as the mean ± the standard error of means (SEMs). Student's t-test was performed. Comparisons of proportions were made using the Fisher exact test. A *P* value below 0.05 was considered statistically significant.

Results

Tumor heterogeneity in N*tv-a* murine models of glioma

Both low-grade and high-grade malignant oligodendrogliomas with features of diffuse infiltration, pseudopallisading necrosis, endothelial cell proliferation, and tracking along white matter fibers were observed in animals that were transfected with PDGF-B or PDGF-B and *Bcl-2* (Fig. 1A). The gliomas expressed GFAP (Fig. 1B). In mice injected with RCAS-PDGF-B alone, 42% (11/26) developed gliomas; and 19% overall (5/26) developed high-grade malignant gliomas. In contrast, when mice were injected with both RCAS-PDGF-B + RCAS-*Bcl-2*, 82% (27/33) developed gliomas, with 61% overall (20/33) being high-grade malignant gliomas (Table 1). In mice that were transfected only with PDGF-B, 81% survived for 90 days at which time the experiment was terminated. In comparison, in mice that were transfected with both PDGF-B + *Bcl-2*, only 44% survived to day 90 (P=0.002)(Fig. 1C). Mice injected with RCAS-Bcl-2 did not develop tumors.

The level of p-STAT3 expression correlates with *in vivo* malignancy and survival

Because a subset of mice that were injected with RCAS-PDGF-B, (an inducer of p-STAT3) and the majority of mice injected with RCAS-PDGF-B + RCAS-*Bcl-2* developed high-grade malignant gliomas, we determined if these tumors demonstrated induction of STAT3. The p-STAT3 expression within tumors in each group was measured using immunohistochemistry and expressed as the percentage of p-STAT3-positive cells (Fig. 2A). We observed p-STAT3 expression in all tumors regardless of model system or grade. Next, we quantified the extent of p-STAT3 expression by counting the number of p-STAT3 positive cells. In the tumors induced by PDGF-B alone, the percentage of cells that expressed p-STAT3 was 27.9 ± 11.1% in high-grade tumors (range 11.5 – 48.8%, n = 3) and 1.0 ± 0.1% in low-grade tumors (range 0.8 – 1.3%, n = 3) (Fig. 2B). In the PDGF-B + *Bcl-2* mice, the percentage of cells that expressed p-STAT3 was 24.1 ± 5.4% in high-grade tumors (range 0.1 – 49.7%, n = 12) and 2.6 ± 1.6% in low grade tumors (range 0.6 – 7.3%, n = 4). The intensity of staining within tumor groups appeared similar.

Given the robust development of high-grade gliomas with marked lethality in the mice injected with RCAS-PDGF-B + RCAS-*Bcl-2*, this particular model system was selected for the analysis of prognostic markers for survival and for treatment studies. The percentage of cells that expressed p-STAT3 was 35.0 ± 4.2% (range 12.9 – 49.7%, n = 8) in mice that died from tumor progression compared with 2.4 ± 1.2% (range 0.1 – 5.4%, n = 4) in long-term survivors (who survived past 90 days and were euthanized without succumbing to their tumor) (Fig. 2C). Indeed, all mice with <10% of cells expressing p-STAT3 survived for the entire 90-day duration, and all mice with cells expressing a p-STAT3 level of >10% died (Fig. 2D).

Intratumoral immunosuppression is prognostic for survival

Because STAT3 is known to regulate Tregs and immunosuppressive macrophages, we next evaluated the presence and prognostic influence of intratumoral immunosuppression. Mice that developed high-grade gliomas developed a marked intratumoral influx of macrophages as determined by F4/80immunohistochemical staining. There was a propensity in the PDGF-B + *Bcl-2* model system for the F4/80-positive cells to co-localize with tumor along the infiltrating subependymal/periventricular edge of the tumors and at markedly higher levels in high-grade tumors than in low-grade tumors, which had few, if any, macrophages (Fig. 3A). In the PDGF-B only mice, macrophage infiltration was 16.2 ± 1.7% (range 13.2 – 19.0%, n = 3) in high-grade tumors and 0.5 ± 0.2% (range 0.3 – 1.0%, n = 3) in low-grade tumors (Fig. 3B). In the PDGF-B + *Bcl-2* group, high-grade tumors showed macrophage infiltration of 25.6 ± 3.8% (range 3.3 – 43.7%, n = 12), whereas low-grade tumors had

macrophage infiltration of 1.7 ± 0.9% (range, 0.3 – 4.0%, n = 5). In the PDGF-B + *Bcl-2* mice with high-grade gliomas, increased macrophage infiltration of their tumors was associated with reduced survival time (Fig. 3C). Among long-term survivors (defined henceforth as mice surviving to 90 days which were euthanized without succumbing to their tumor), infiltration of F4/80-positive macrophages was 11.3 ± 3.8% (range 3.3 – 19.5%, n = 4), whereas in the mice that succumbed to intracranial tumors prior to 90 days, there was a macrophage infiltration of 32.8 ± 3.2% (range 21.7 – 43.7%, n = 8). Indeed, all mice with macrophage infiltration of <20% survived for the entire 90-day duration, and all mice with macrophage infiltration of >20% died (Fig. 3D).

Treg infiltration was determined using immunohistochemical staining for FoxP3. Similar levels of infiltration by FoxP3-positive cells were seen in both high- and low-grade tumors (Fig. 4A). In the PDGF-B only mice, Treg infiltration was 5.7 ± 0.1% (range 5.4 – 5.9, n = 3) in high-grade tumors and 3.5 ± 0.8% (range 2.2 – 5.0, n = 3) in low-grade tumors (Fig. 4B). In the PDGF-B + Bcl2 mice, high-grade tumors had Treg infiltration of 3.6 ± 0.4% (range 2.0 – 6.4%, n = 12), whereas low-grade tumors had Treg infiltration of 2.8 ± 0.3% (range 2.1 – 3.0, n = 3). In the PDGF-B + *Bcl-2* mice with high-grade gliomas, increased infiltration of the tumors by the Tregs was not associated with decreased survival time (Fig. 4C). Among long-term survivors, infiltration of FoxP3-positive cells was 3.6 ± 0.6% (range 2.9 – 5.1%, n = 4), whereas in the mice that succumbed to intracranial tumors prior to 90 days, the FoxP3-positive cells was 3.6 ± 0.7% (range 2.0 – 6.4%, n = 8). There was no correlation between the number of FoxP3-positive cells and survival duration (Fig. 4D).

WP1066 inhibits intratumoral immunosuppression that correlates with treatment response

Because co-expression of RCAS-PDGF-B and RCAS-*Bcl-2* in Ntv-a mice induces tumors that express p-STAT3 and have a high-incidence of glioma formation, this model was utilized to test the feasibility of ascertaining the *in vivo* efficacy of WP1066. Treatment with WP1066 (o.g.) commenced on day 21 after the RCAS vector injection. The median survival time for the control group was 57 days, whereas for mice treated with WP1066, the median survival times were more than 90 days (P=0.07) in comparison to the vehicle control treated mice (Fig. 5A and summarized in Table 2). For the mice treated by o.g. with WP1066 at a dose of 40 mg/kg (n=15), 73% survived long term (>90 days) (*Chi-square* P=0.07 relative to the control group in which 40% survived long term), and there was at least a 58% increase in median survival time when the experiment was terminated at 90 days (Fig. 5A). In addition, after 90 days, all 11/15 (73.3%) of the surviving mice treated with WP1066 had no evidence of any intracranial tumor on histopathological examination compared with 5/15 (33.3%, P=0.03) of the control mice. High-grade tumors developed in 1/15 (6.7%) of the WP1066 treated mice relative to 4/15 (26.7%) in the control mice (P=0.16). The tumors in the mice treated with WP1066 showed a marked decrease in p-STAT3 expression (3.6 ± 1.6%, range 0.6 – 5.9%, n = 3) compared with the untreated mice (36.3 ± 10.6%, range 6.1 – 51.5, n = 4, P = 0.05) (Fig. 5B). Similarly, WP1066 also decreased macrophage infiltration of tumors, with treated mice having 5.0 ± 3.3% F4/80-positive cells (range 1.6 – 11.5, n = 3) compared with 17.4 ± 4.9 (range 6.0 – 26.9%, n = 4, P = 0.05) in control mice (Fig. 5C). WP1066 did not affect Treg infiltration of tumors, with treated mice having 6.1 ± 3.7% FoxP3-positive cells (range 0.7 – 13.3%, n = 3) compared with 6.1 ± 2.0% (range 1.6 – 12.8%, n = 5, P = 0.99) in control mice (Fig. 5D).

Discussion

There are several distinctive and novel findings in this study. The first is that WP1066 is demonstrating efficacy in a heterogeneous, orthotopic glioma model system. Utilizing the RCAS/Ntv-a system, we demonstrated that the histopathological characterization of the tumors produced recapitulated many of the fundamental characteristics seen in human high-

grade gliomas, including pseudopallisading necrosis, infiltration along white matter tracts, and diffuse infiltration. Previous preclinical studies of the effects of WP1066 on gliomas were confined to a clonotypic glioma in a non orthotopic position in an immunosuppressed murine model (36). Secondly, WP1066 is exerting a therapeutic effect on oligodendrogliomas, which has not been previously described. Finally, we are not aware of any previous attempts at correlating a novel, murine model system, including tumor-mediated immune suppression mechanisms, with human immune prognostic biology in the context of an immune therapeutic strategy. Specifically, we demonstrated that the expression *in vivo* of STAT3 in the RCAS-PDGF-B and RCAS-PDGF-B + RCAS-*Bcl-2* models of glioma correlated with glioma grade and prognosis, similar to the findings in human glioma patients (19). Additionally, the murine gliomas also demonstrated an influx of macrophages that correlated with grade and prognosis seen in human glioma patients (50–53). These tumor-associated macrophages have previously been shown to enhance tumorigenesis, invasion and angiogenesis in the tumor microenvironment (27,54–57). There was a propensity of the macrophages to distribute in the subependymal region in the murine models, likely related to the mechanism of induction of tumor, in contrast to the localization of macrophages in regions of pseudopallisading necrosis commonly seen in human gliomas. Finally, we found FoxP3-positive cells were present, albeit low at 6%, within the murine glioma microenvironment that did not correlate with grade and was not a prognostic marker that was markedly comparable to the findings in human patients with oligodendrogliomas (58). It is possible that the FoxP3 expression was occurring within the cancer cells (59); however we confined our counts to those cells that had a lymphocyte morphology. These data, in conjunction with another study showing that the immune infiltration in spontaneous mouse astrocytomas evolved along with the stages of tumor development (60) indicate that these murine model systems may be suitable for the study of immunotherapeutic approaches because many features of tumor-mediated immunosuppression observed in these systems appear similar to those seen in human glioma patients.

The STAT3 inhibitor WP1066 exerted a therapeutic benefit, inhibited intratumoral p-STAT3 expression, and suppressed intratumoral macrophage infiltration that correlated with treatment response. Although FoxP3 expression is under transcriptional control of STAT3 (61,62) and WP1066 has been previously shown to inhibit Tregs in the systemic circulation (30,63), we did not find a decrease in the level of FoxP3 expression during treatment with WP1066. The failure of WP1066 to further decrease the numbers of FoxP3 expressing cells in the oligodendroglial-like tumors in this animal model system may simply reflect the low baseline levels. Although p-STAT3 is not ubiquitously expressed in all tumor cells in the murine model system, there is nonetheless marked *in vivo* efficacy. This discrepancy can be resolved by the activity of WP1066 exerting both direct effects on tumor cells expressing p-STAT3 and the immune cells expressing p-STAT3, which restrains their anti-tumor activity including recognition of tumor-associated and tumor-specific antigens. The inhibition of p-STAT3 restores anti-tumor immune clearance (28,64), and therefore we suspect that WP1066 exerts a bystander effect on p-STAT3 negative-expressing cells by eradicating those tumor cells that can by immunologically recognized. This contention is supported by the fact that therapeutic efficacy of WP1066 is lost in nude models systems and with *in vivo* depletions of the CD4 and CD8 subpopulations (unpublished data).

A confounding problem in the use of these model systems is that tumor incidence is not 100%, and thus a randomization schema is necessary. Furthermore, it is unpredictable which mice develop tumors, the exact onset of tumor development, and the pathological grade at the time of treatment initiation. Finally, because the transgenes are introduced in the neonatal period, onset of treatment also needs to be stratified and/or randomized based on age because most facilities would be unlikely to be able to accommodate sufficient breeding pairs to have adequate numbers of animals for entry into treatment groups. This did not pose

a significant hardship in the current studies in which only two experimental cohorts were utilized; however, for much more complex immunotherapeutic efficacy trials, especially those involving combinational approaches, this will introduce complexity in the design. A recent study by Singh et al., proposed that the use of genetically engineered murine models may more reliably predict human clinical outcomes (8). In the context of their study, a correlation was made with chemotherapeutics. We now propose that these genetically engineered murine models may also be suitable for the testing of immunotherapeutics based, in part, on the biology recapitulating many of the hallmark features of high-grade gliomas, on the correlative nature of the immunosuppressive biology, and specifically, the intratumoral biology.

Statement of Translational Relevance

Murine models utilized for the pre-clinical assessment of therapeutics are inconsistently predictive of human clinical responses due to the clonotypic nature of xenografted cell-lines and the use of immune-compromised animals. These models fail to recapitulate the heterogeneous biology and immunosuppression seen in human disease. Thus, immunocompetent murine models are necessary for the investigation of *in vivo* tumor-mediated immunosuppression and the evaluation of immunotherapeutics. This study demonstrates that in immunocompetent mice that develop endogenous high-grade gliomas that recapitulate many of the phenotypic and immunologic features of de novo human gliomas, the degree of immunosuppression as determined by the level of intratumoral signal transducer and activator of transcript (STAT3) expression and macrophage infiltration has prognostic significance. When animals were treated with a STAT3 inhibitor, both intratumoral STAT3 expression and macrophage infiltration were decreased, which correlated with increased survival. These findings demonstrate the importance of immunocompetent animal model systems to appropriately assess the impact of tumor-mediated immunosuppression in gliomagenesis and to evaluate novel immunotherapeutic strategies.

Abbreviations used

CNS	Central nervous system
STAT3	transducer and activator of transcription 3

Acknowledgments

We thank Audria Patrick and David M. Wildrick, Ph.D., for editorial assistance.

Grant Support

This work was supported by The Brain Tumor Society, the Anthony Bullock III Foundation (ABH), the Mitchell Foundation (ABH), the Dr. Marnie Rose Foundation (ABH), and the U. S. National Institutes of Health grants CA120813-03, A177225-01, P50 CA093459 (ABH), P50CA127001 (GR) and P50 CA093459 (WP). The funding organizations had no role in the study design, data collection and analysis, decision to publish, or preparation of the manuscript.

References

1. Fomchenko EI, Holland EC. Mouse models of brain tumors and their applications in preclinical trials. Clin Cancer Res 2006;12:5288–5297. [PubMed: 17000661]
2. Sharpless NE, Depinho RA. The mighty mouse: genetically engineered mouse models in cancer drug development. Nat Rev Drug Discov 2006;5:741–754. [PubMed: 16915232]

3. Hatiboglu AM, Wei J, Wu A, Heimberger AB. Immune therapeutic targeting of glioma cancer stem cells. Targeted Oncology. In Press.
4. Holland EC, Celestino J, Dai C, Schaefer L, Sawaya RE, Fuller GN. Combined activation of Ras and Akt in neural progenitors induces glioblastoma formation in mice. Nat Genet 2000;25:55–57. [PubMed: 10802656]
5. Zheng H, Ying H, Yan H, et al. p53 and Pten control neural and glioma stem/progenitor cell renewal and differentiation. Nature 2008;455:1129–1133. [PubMed: 18948956]
6. Huse JT, Holland EC. Genetically engineered mouse models of brain cancer and the promise of preclinical testing. Brain Pathol 2009;19:132–143. [PubMed: 19076778]
7. Francia G, Kerbel RS. Raising the bar for cancer therapy models. Nature Biotechnology 2010;28:561–562.
8. Singh M, Lima A, Molina R, et al. Assessing therapeutic responses in Kras mutant cancers using genetically engineered mouse models. Nat Biotechnol 28:585–593. [PubMed: 20495549]
9. Fleming TP, Saxena A, Clark WC, et al. Amplification and/or overexpression of platelet-derived growth factor receptors and epidermal growth factor receptor in human glial tumors. Cancer Res 1992;52:4550–4553. [PubMed: 1322795]
10. Thorarinsdottir HK, Santi M, McCarter R, et al. Protein expression of platelet-derived growth factor receptor correlates with malignant histology and PTEN with survival in childhood gliomas. Clin Cancer Res 2008;14:3386–3394. [PubMed: 18519768]
11. Potapova O, Fakhrai H, Baird S, Mercola D. Platelet-derived growth factor-B/v-sis confers a tumorigenic and metastatic phenotype to human T98G glioblastoma cells. Cancer Res 1996;56:280–286. [PubMed: 8542581]
12. Lindberg N, Kastemar M, Olofsson T, Smits A, Uhrbom L. Oligodendrocyte progenitor cells can act as cell of origin for experimental glioma. Oncogene 2009;28:2266–2275. [PubMed: 19421151]
13. Doucette T, Yang Y, Zhang W, et al. Bcl-2 Promotes Malignant Progression in Oligodendroglioma. Submitted.
14. Dunlap SM, Celestino J, Wang H, et al. Insulin-like growth factor binding protein 2 promotes glioma development and progression. Proc Natl Acad Sci U S A 2007;104:11736–11741. [PubMed: 17606927]
15. Huse JT, Brennan C, Hambardzumyan D, et al. The PTEN-regulating microRNA miR-26a is amplified in high-grade glioma and facilitates gliomagenesis in vivo. Genes Dev 2009;23:1327–1337. [PubMed: 19487573]
16. Wang YZ, Wharton W, Garcia R, Kraker A, Jove R, Pledger WJ. Activation of Stat3 preassembled with platelet-derived growth factor beta receptors requires Src kinase activity. Oncogene 2000;19:2075–2085. [PubMed: 10815799]
17. Bowman T, Broome MA, Sinibaldi D, et al. Stat3-mediated Myc expressionis required for Src transformation and PDGF-induced mitogenesis. Proc Natl Acad Sci U S A 2001;98:7319–7324. [PubMed: 11404481]
18. Winston LA, Hunter T. JAK2, Ras, and Raf are required for activation of extracellular signal-regulated kinase/mitogen-activated protein kinase by growth hormone. J Biol Chem 1995;270:30837–30840. [PubMed: 8537333]
19. Abou-Ghazal M, Yang DS, Qiao W, et al. The incidence, correlation with tumor-infiltrating inflammation, and prognosis of phosphorylated STAT3 expression in human gliomas. Clin Cancer Res 2008;14:8228–8235. [PubMed: 19088040]
20. Alas S, Bonavida B. Rituximab Inactivates Signal Transducer and Activation of Transcription 3 (STAT3) Activity in B-Non-Hodgkin's Lymphoma through Inhibition of the Interleukin 10 Autocrine/Paracrine Loop and Results in Down-Regulationof Bcl-2 and Sensitization to Cytotoxic Drugs. Cancer Res 2001;61:5137–5144. [PubMed: 11431352]
21. Bhattacharya S, Ray RM, Johnson LR. STAT3-mediated transcription of Bcl-2, Mcl-1 and c-IAP2 prevents apoptosis in polyamine-depleted cells. Biochem J 2005;392:335–344. [PubMed: 16048438]
22. Nielsen M, G KC, W EK, et al. Inhibition of constitutively activated Stat3 correlates with altered Bcl-2/Bax expression and induction of apoptosis in mycosis fungoides tumor cells. Leukemia 1999;13:735–738. [PubMed: 10374878]

23. Jarnicki A, Putoczki T, Ernst M. Stat3: linking inflammation to epithelial cancer - more than a "gut" feeling? Cell Div 5:14. [PubMed: 20478049]
24. Yu H, Kortylewski M, Pardoll D. Crosstalk between cancer and immune cells: role of STAT3 in the tumour microenvironment. Nat Rev Immunol 2007;7:41–51. [PubMed: 17186030]
25. O'Farrell AM, Liu Y, Moore KW, Mui AL. IL-10 inhibits macrophage activation and proliferation by distinct signaling mechanisms: Evidence for Stat3-dependent and independent pathways. EMBO J 1998;17:1006–1018. [PubMed: 9463379]
26. Mancino A, Lawrence T. Nuclear factor-kappaB and tumor-associated macrophages. Clin Cancer Res 2010;16:784–789. [PubMed: 20103670]
27. Wu A, Wei J, Kong LY, et al. Glioma cancer stem cells induce immunosuppressive macrophages/microglia. Neuro Oncol.
28. Kortylewski M, Kujawski M, Wang T, et al. Inhibiting Stat3 signaling in the hematopoietic system elicits multicomponent antitumor immunity. Nat Med 2005;11:1314–1321. [PubMed: 16288283]
29. Zorn E, Nelson EA, Mohseni M, et al. IL-2 regulates FOXP3 expression in human CD4+CD25+ regulatory T cells through a STAT-dependent mechanism and induces the expansion of these cells in vivo. Blood 2006;108:1571–1579. [PubMed: 16645171]
30. Kong L-K, Wei J, Sharma AK, et al. A novel phosphorylated STAT3 inhibitor enhances T cell cytotoxicity against melanoma through inhibition of regulatory T cells. Cancer Immunol Immunother 2008;58:1023–1032. [PubMed: 19002459]
31. Sherry MM, Reeves A, Wu JK, Cochran BH. STAT3 is required for proliferation and maintenance of multipotency in glioblastoma stem cells. Stem Cells 2009;27:2383–2392. [PubMed: 19658181]
32. Wei J, Bar J, Kong L-Y, et al. Glioblastoma cancer-initiating cells inhibit T cell proliferation and effector responses by the STAT3 pathway. Mol Cancer Ther 2010;9:67–78. [PubMed: 20053772]
33. Horiguchi A, Asano T, Kuroda K, et al. STAT3 inhibitor WP1066 as a novel therapeutic agent for renal cell carcinoma. Br J Cancer 102:1592–1599. [PubMed: 20461084]
34. Kong LY, Abou-Ghazal MK, Wei J, et al. A novel inhibitor of signal transducers and activators of transcription 3 activation is efficacious against established central nervous system melanoma and inhibits regulatory T cells. Clin Cancer Res 2008;14:5759–5768. [PubMed: 18794085]
35. Ferrajoli A, Faderl S, Van Q, et al. WP1066 disrupts Janus kinase-2 and induces caspase-dependent apoptosis in acute myelogenous leukemia cells. Cancer Res 2007;67:11291–11299. [PubMed: 18056455]
36. Iwamaru A, Szymanski S, Iwado E, et al. A novel inhibitor of the STAT3 pathway induces apoptosis in malignant glioma cells both in vitro and in vivo. Oncogene 2007;26:2435–2444. [PubMed: 17043651]
37. Kupferman ME, Jayakumar A, Zhou G, et al. Therapeutic suppression of constitutive and inducible JAK\STAT activation in head and neck squamous cell carcinoma. J Exp Ther Oncol 2009;8:117–127. [PubMed: 20192118]
38. Hussain SF, Kong L-Y, Jordan J, et al. A novel small molecule inhibitor of signal transducers and activators of transcription 3 reverses immune tolerance in malignant glioma patients. Cancer Res 2007;67:9630–9636. [PubMed: 17942891]
39. Wu A, Wei J, Kong LY, et al. Glioma cancer stem cells induce immunosuppressive macrophages/microglia. Neuro Oncol. In Press.
40. Uhrbom L, Dai C, Celestino JC, Rosenblum MK, Fuller GN, Holland EC. Ink4a–Arf loss cooperates with KRas activation in astrocytes and neural progenitors to generate glioblastomas of various morphologies depending on activated Akt. Cancer Res 2002;62:5551–5558. [PubMed: 12359767]
41. Ferletta M, Uhrbom L, Olofsson T, Ponten F, Westermark B. Sox10 has a broad expression pattern in gliomas and enhances platelet-derived growth factor-B--induced gliomagenesis. Mol Cancer Res 2007;5:891–897. [PubMed: 17855658]
42. Fults D, Pedone C, Dai C, Holland EC. MYC expression promotes the priliferation of neural progenitor cells in culture and in vivo. Neoplasia 2002;4:32–39. [PubMed: 11922389]
43. Moore LM, Holmes KM, Smith SM, et al. IGFBP2 is a candidate biomarker for Ink4a–Arf status and a therapeutic target for high-grade gliomas. Proc Natl Acad Sci U S A 2009;106:16675–16679. [PubMed: 19805356]

44. McCall TD, Pedone CA, Fults DW. Apoptosis suppression by somatic cell transfer of Bcl-2 promotes Sonic hedgehog-dependent medulloblastoma formation in mice. Cancer Res 2007;67:5179–5185. [PubMed: 17545597]
45. Dai C, Celestino JC, Okada Y, Louis DN, Fuller GN, Holland EC. PDGF autocrine stimulation dedifferentiates cultured astrocytes and induces oligodendrogliomas and oligoastrocytomas from neural progenitors and astrocytes in vivo. Genes Dev 2001;15:1913–1925. [PubMed: 11485986]
46. Holland EC, Varmus HE. Basic fibroblast growth factor induces cell migration and proliferation after glia-specific gene transfer in mice. Proc Natl Acad Sci U S A 1998;95:1218–1223. [PubMed: 9448312]
47. Binning MJ, Niazi T, Pedone CA, et al. Hepatocyte growth factor and sonic Hedgehog expression in cerebellar neural progenitor cells costimulate medulloblastoma initiation and growth. Cancer Res 2008;68:7838–7845. [PubMed: 18829539]
48. Kaplan EL, Meier P. Nonparametric estimation from incomplete observations. J Am Stat Assoc 1958;53:457–481.
49. Mantel N. Evaluation of survival data and two new rank order statistics arising in its consideration. Cancer Chemother Rep 1966;50:163–170. [PubMed: 5910392]
50. Hussain SF, Yang D, Suki D, Aldape K, Grimm E, Heimberger AB. The role of human glioma-infiltrating microglia/macrophages in mediating antitumor immune responses. Neuro Oncol 2006;8:261–279. [PubMed: 16775224]
51. Komohara Y, Ohnishi K, Kuratsu J, Takeya M. Possible involvement of the M2 anti-inflammatory macrophage phenotype in growth of human gliomas. J Pathol 2008;216:15–24. [PubMed: 18553315]
52. Rodero M, Marie Y, Coudert M, et al. Polymorphism in the microglial cell-mobilizing CX3CR1 gene is associated with survival in patients with glioblastoma. J Clin Oncol 2008;26:5957–5964. [PubMed: 19001328]
53. Sliwa M, Markovic D, Gabrusiewicz K, et al. The invasion promoting effect of microglia on glioblastoma cells is inhibited by cyclosporin A. Brain 2007;130:476–489. [PubMed: 17107968]
54. Bingle L, Brown NJ, Lewis CE. The role of tumour-associated macrophages in tumour progression: implications for new anticancer therapies. J Pathol 2002;196:254–265. [PubMed: 11857487]
55. Mantovani A, Bottazzi B, Colotta F, Sozzani S, Ruco L. The origin and function of tumor-associated macrophages. Immunol Today 1992;13:265–270. [PubMed: 1388654]
56. Niu G, Briggs J, Deng J, et al. Signal transducer and activator of transcription 3 is required for hypoxia-inducible factor-1alpha RNA expression in both tumor cells and tumor-associated myeloid cells. Mol Cancer Res 2008;6:1099–1105. [PubMed: 18644974]
57. Pollard JW. Tumour-educated macrophages promote tumour progression and metastasis. Nat Rev Cancer 2004;4:71–78. [PubMed: 14708027]
58. Heimberger AB, Reina-Ortiz C, Yang DS, et al. Incidence and prognostic impact of FoxP3+ regulatory T cells in human gliomas. Clin Cancer Res 2008;14:5166–5172. [PubMed: 18698034]
59. Karanikas V, Speletas M, Zamanakou M, et al. Foxp3 expression in human cancer cells. J Transl Med 2008;6:19. [PubMed: 18430198]
60. Tran Thang NN, Derouazi M, Philippin G, et al. Immune infiltration of spontaneous mouse astrocytomas is dominated by immunosuppressive cells from early stages of tumor development. Cancer Res 2010;70:4829–4839. [PubMed: 20501837]
61. Zorn E, Nelson EA, Mohseni M, et al. IL-2 regulates FOXP3 expression in human CD4+CD25+ regulatory T cells through a STAT-dependent mechanism and induces the expansion of these cells in vivo. Blood 2006;108:1571–1579. [PubMed: 16645171]
62. Kortylewski M, Xin H, Kujawski M, et al. Regulation of the IL-23 and IL-12 balance by Stat3 signaling in the tumor microenvironment. Cancer Cell 2009;15:114–123. [PubMed: 19185846]
63. Kong LY, Gelbard A, Wei J, et al. Inhibition of p-STAT3 enhances IFN-α efficacy against metastatic melanoma. Clin Cancer Res. 2010
64. Albesiano E, Davis M, See AP, et al. Immunologic consequences of signal transducers and activators of transcription 3 activation in human squamous cell carcinoma. Cancer Res 70:6467–6476. [PubMed: 20682796]

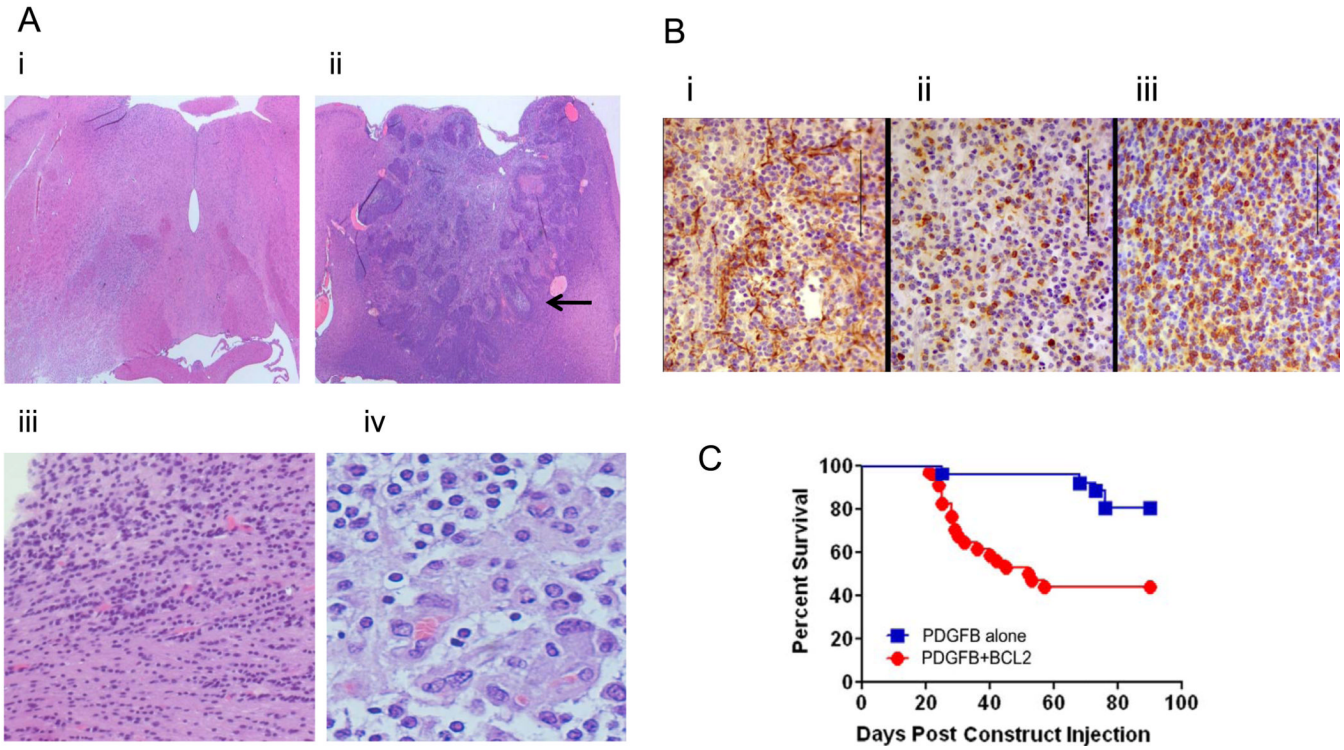

Fig. 1.

(**A**) Representative hematoxylin and eosin stained light microscopy images showing the phenotypic features of *de novo* (i) low- (50X) and (ii) high-grade gliomas (50X) in the PDGF-B + *Bcl-2* mouse, including (i, ii) diffuse infiltration, (ii) pseudopallisading necrosis (arrow demonstrating), (iii) white matter tracking (100X), and (iv) vascular proliferation (400X). (**B**) The induced tumors in the PDGF-B + Bcl-2 mice demonstrating positive expression of (i) GFAP, the (ii) the hemagluttinin epitope tag (detecting PDGF-B expression), and (iii) Bcl-2 (400X; scale bar = 100 μm). (**C**) Kaplan-Meier survival curves showing overall survival of PDGF-B alone, and PDGF-B + *Bcl-2* mice. Median survival was longer than 90 days in the PDGF-B alone mice and 52.5 days in the PDGF-B + *Bcl-2* mice ($P = 0.005$) (Animals surviving for longer than 90 days were terminated for histopathological tissue examination and analysis.)

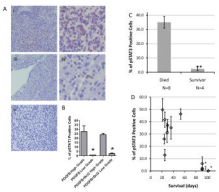

Fig. 2.

(**A**) Representative light microscopy images showing immunohistochemical staining for p-STAT3 in a high-grade glioma at (i) low (100X) and (ii) high (400X) magnification, and in a low-grade tumor at (iii) low (100X) and (iv) high (400X) magnification, and (v) rabbit IgG isotype control (100X). (**B**) In the PDGF-B alone, and PDGF-B + *Bcl-2* mice that developed gliomas, p-STAT3 levels were significantly higher in high-grade tumors than in low-grade tumors (* $P < 0.05$). (**C**) In PDGF-B + *Bcl-2* mice with high-grade gliomas, animals that survived past 90 days had significantly lower tumor p-STAT3 expression than animals that succumbed to intracranial tumors before 90 days (** $P < 0.0001$). (**D**) Mean p-STAT3 expression in individual mice in the PDGF-B + Bcl2 group bearing high-grade tumors plotted against overall survival time showing long-term survival of all animals with p-STAT3 expression that was < 10%. (* = animals sacrificed after surviving past 90 days. Error bars represent standard error of the mean.)

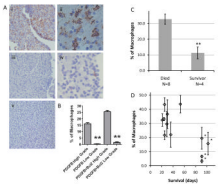

Fig. 3.

(**A**) Representative light microscopy images showing immunohistochemical staining of F4/80 to identify infiltrating macrophages/microglia in a high-grade tumor at (i) low (100X) and (ii) high (400X) magnification, and a low-grade tumor at (iii) low (100X) and (iv) high (400X) magnification, and (v) rat IgG isotype control (100X). (**B**) In the PDGF-B alone, and PDGF-B + *Bcl-2* mice, macrophage infiltration was significantly higher in high-grade tumors than in low-grade tumors (** $P < 0.05$). (**C**) In PDGF-B + *Bcl-2* mice with high-grade gliomas that survived past 90 days had significantly lower levels of macrophage infiltration than those that succumbed to intracranial tumors before 90 days (** $P = 0.003$). (**D**) Mean degree of macrophage infiltration in individual mice in the PDGF-B + *Bcl2* group bearing high-grade tumors plotted against overall survival time, showing long-term survival of all animals with macrophage infiltration of < 20%. (* = animals sacrificed after surviving past 90 days. Error bars represent standard error of the mean.)

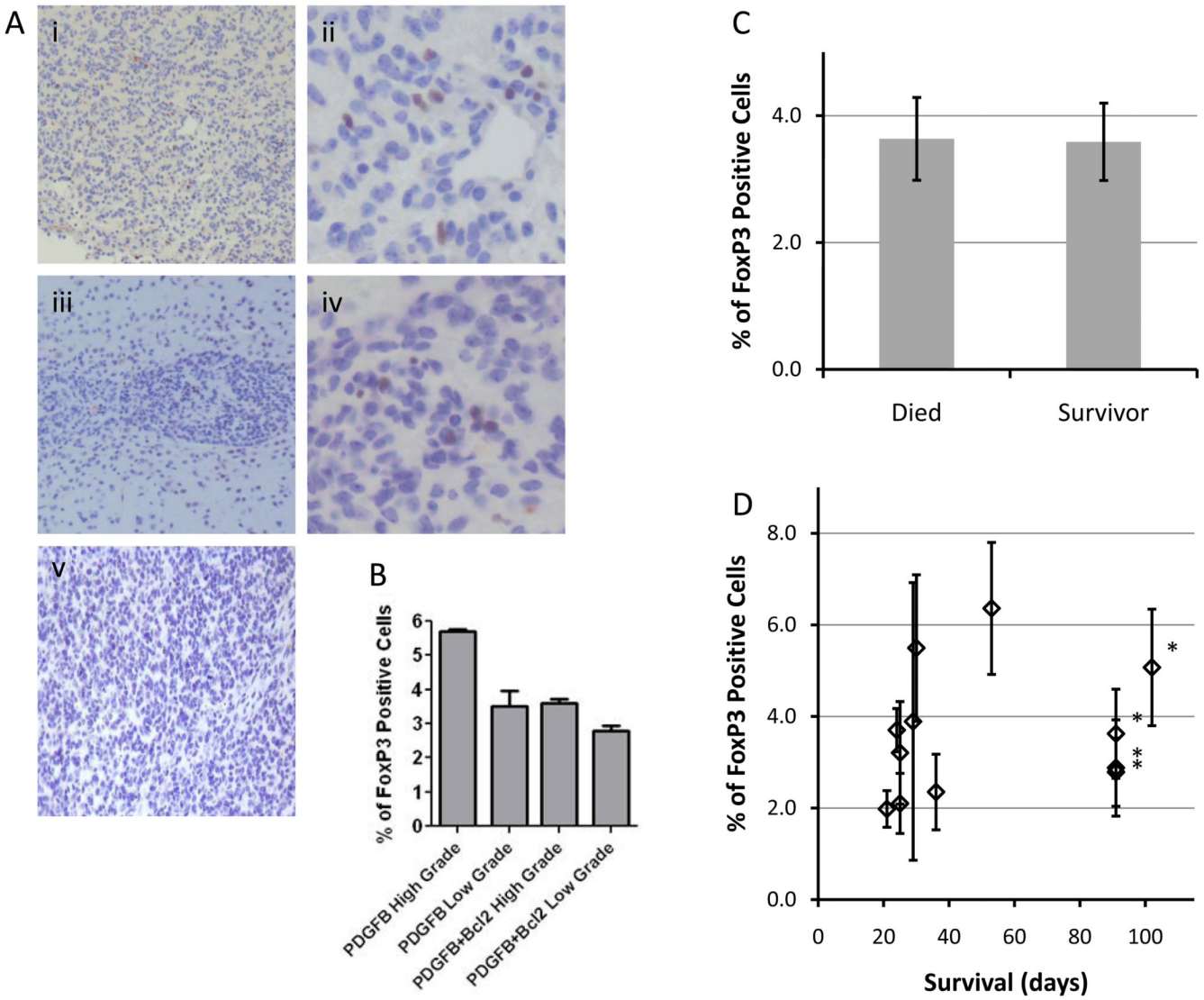

Fig. 4.

(**A**) Representative light microscopy images showing immunohistochemical staining of FoxP3 to identify infiltrating Tregs in a high-grade tumor at (i) low (100X) and (ii) high (400X) magnification, and a low-grade tumor at (iii) low (100X) and (iv) high (400X) magnification, and (v) mouse IgG isotype control (100X). (**B**) In the PDGF-B alone, and PDGF-B + *Bcl-2* mice, the level of Treg infiltration was observed to be similar in high- and low-grade tumors. (**C**) In the PDGF-B + Bcl2 group, no significant differences were observed in mean levels of Treg infiltration between mice with high-grade gliomas who survived longer than 90 days and those that succumbed to intracranial tumors before 90 days. (**D**) In the PDGF-B + *Bcl2* group, the mean degree of Treg infiltration in individual high-grade tumor bearing mice did not correlate with length of survival.

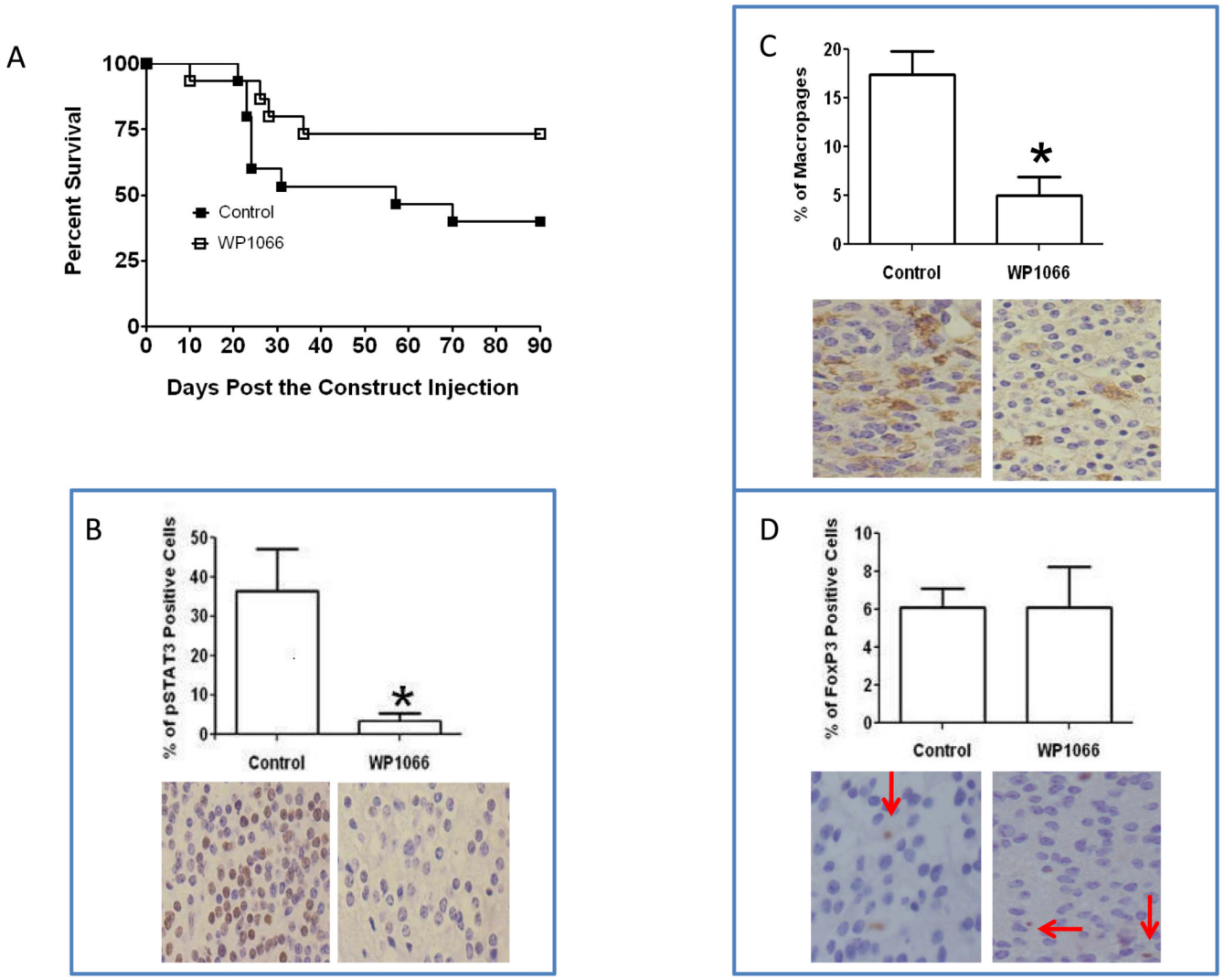

Fig. 5.

(**A**) Kaplan-Meier survival curve showing improved survival in PDGF-B and *Bcl-2* mice treated with the p-STAT3 inhibitor WP1066 compared with untreated controls. (**B**) WP1066 treatment significantly reduced levels of p-STAT3 expression. Representative light microscopy images show immunohistochemistry of p-STAT3 (brown nuclear staining) in a high-grade glioma from a vehicle control mouse and a WP1066-treated mouse (400X). (**C**) WP1066 also suppressed F4/80-positive macrophage infiltration. Representative light microscopy images showing immunohistochemistry of F4/80 (brown cytoplasmic staining) demonstrating infiltrating macrophages/microglia in a high-grade glioma from a vehicle control mouse and a WP1066-treated mouse (400X). (**D**) WP1066 did not suppress the number of intratumoral FoxP3-positive cells. Representative light microscopy images showing immunohistochemistry of FoxP3 (brown staining) from a vehicle control mouse and a WP1066-treated mouse (400X). (* $P < 0.05$).

Table 1

Characteristics of induced gliomas

		High-grade glioma	Low-grade glioma
Key histological features		Anaplasia Mitotic activity Microvascular proliferation Pseudopallisading necrosis	No anaplasia Minimal mitotic activity No microvascular proliferation No necrosis
Equivalent human grade		WHO grade III	WHO grade II
Equivalent human pathology		Anaplastic Oligodendroglioma	Oligodendroglioma
PDGF-B murine system	Incidence of gliomas	19% (5/26)	81% (21/26)
	GFAP staining	Positive	Positive
	Mitotic index	1.8%	0.9%
	Bcl-2 staining	Minimal	Minimal
	% cells expressing p-STAT3	27.9 ± 11.1%	1.0 ± 0.1%
	% of macrophages	16.2 ± 1.7%	0.5 ± 0.2%
	% of FoxP3 positive cells	5.7 ± 0.1%	3.5 ± 0.8%
PDGF-B + *BCL-2* murine system	Incidence of gliomas	61% (20/33)	39% (13/33)
	GFAP staining	Positive	Positive
	Mitotic index	11.0%	1.0%
	Bcl-2 staining	High	Minimal
	% cells expressing p-STAT3	24.1 ± 5.4%	2.6 ± 1.6%
	% of macrophages	25.6 ± 3.8%	1.7 ± 0.9%
	% of FoxP3 positive cells	3.6 ± 0.4%	2.8 ± 0.3%

Table 2

Treatment response of WP1066-treated RCAS-PDGF-B + RCAS-BCL-2 induced gliomas.

	Control	WP1066
Median survival	57 days	>90 days
Development of high-grade gliomas on day 90	26.7%	6.7%
% of p-STAT3 expressing cells	36.3 ± 10.6%	3.6 ± 1.6%
% of macrophages	17.4 ± 4.9%	5.0 ± 3.3%
% of Tregs	6.1 ± 2.0%	6.1 ± 3.7%